Sudan University of Sciences and Technology
College of Graduate Studies

Characterization of Brain Tumors in Magnetic Resonance Images Using Texture Analysis

توصيف أورام الدماغ في صور الرنين المغناطيسي باستخدام تحليل النسيج

Thesis Submitted for partial fulfillment for The Requirement M.Sc. Degree in medical physics

By:

Alabbas Abdalhafeez Ibrahim Saeed

Supervisor:

Dr. Hussein Ahmed Hassan

2020

الآية

بسم الله الرحمن الرحيم

قَالَ تَعَالَىٰ:

﴿ قَالَ لَهُۥ مُوسَىٰ هَلۡ أَتَّبِعُكَ عَلَىٰٓ أَن تُعَلِّمَنِ مِمَّا عُلِّمۡتَ رُشۡدٗا ٦٦ ﴾

سورة الكهف : الاية 66

Dedication

To my father

To my mother

To all my family, And to my friends

Acknowledgement

I would like to express my sincere gratitude to my supervisor for his helpful guidance and continuous support.

I would also like to thank the rest of thesis committee. And all those who helped make this work possible.

I also would like to thank Mrs/ Jwyria Eltayeb Ahmed Mohammed

Deep thank to Dr/ Mazan Mahmoud and Mr salim

Abstract

This study was carried out in order to characterize of brain tumor in MRI by applying texture analysis to the brain tissues represented on MRI to recognizes the brain tumors from the other brain tissues which included: grey and white matter, fatty tissue, CSF and brain tumor. This study was carried out in the period from April 2020 to October 2020 in Khartoum state at Antalya diagnostic center. The images were obtained by (Signa HDxt 1.5 Tesla MRI systems). The data of this study collected from 50 patients having axial views that include brain tumor and they were selected randomly from a set of 50 MR images from 5 patients. the data were extracted from the image using 3×3 pixels window inside the window the first order and second order statistics were calculated and used to classify the brain MRI into one of the four tissues mentioned earlier. The window scans the whole image by interlacing it one pixel horizontally, then start again from the send line when the above one was completed till the end of the image. The results of this study showed that the overall accuracy of classification process was 94.8% and for the tumor the sensitivity was 80.8% white matter and grey matter showed a classification accuracy of 89.6% and for CSF was 82.5% and fatty tissue 71.9%. In conclusion these results showed that brain tumor can be classified successfully and delineated using texture analysis with a minimum effort.

المستخلص

اجريت هذه الدراسة بهدف توصيف الورم الدماغي بالتصوير بالرنين المغنطيسي من خلال تطبيق التحليل النسيجي لانسجة المخ، لتمييز اورام الدماغ من انسجة المخ الاخرى التي شملت المادة الرمادية و البيضاء و الانسجة الدهنية و السائل النخاعي الدماغي. و قد اجريت هذه الدراسة في الفترة من ابريل 2020 الى اكتوبر 2020، في مركز انطاليا التشخيصي بالخرطوم، تم اخذ الصور بواسطة نظام سيغنا اتش دي اكس تي و جمعت بيانات الدراسة من حوالي 50 صورة ل5 مرضى من مقطع محوري، متضمنة اورام الدماغ وتم اختيارها بطريقة عشوائية من مجموعة قوامها 50 حالة مرضية. البيانات استخلصت من صور الرنين المغنطيسي 3*3 وحدة داخل نافذة حسابات الاحصاء من الدرجة الاولى و الثانية، و الذي استخدم لتصنيف صور الرنين المغنطيسي المأخوذة للدماغ لتمييز كل واحدة من الانسجة الخمسة المذكورة اعلاه. اظهرت نتائج الدراسة ان الدقة الشاملة في عملية التصنيف كانت 94.8% و بالنسبة لاورام الدماغ الحساسية 80.8% و اظهرت المادة البيضاء و الرمادية دقة التصنيف 89.6% و السائل النخاعي الدماغي كانت 82.5% و النسيج الدهني 71.9%، و في ختام اظهرت هذه النتائج ان ورم المخ يمكن تصنيفه بنجاح و تخطيطه باستخدام التحليل النسيجي باقل جهد ممكن.

Table of Content

Table of figures

Table of tables

Chapter One
1. Introduction

Chapter One

1. Introduction

1.1. Texture analysis in quantitative MR imaging: tissue characterization of normal brain and intracranial tumors at 1.5T

1. Introduction

Brain neoplasms or intracranial tumors, which is more common in older adults, can affect individuals of any age including pediatric and children. Exposure to carcinogenic agents including ionizing radiation and family history are among the main causes of the disease. Early diagnosis is crucial to avoid prolonged period of morbidity and help in reduction of mortality rate by avoiding life threatening complications and providing effective treatment on time.

When the mechanisms controlling the growth of normal cells fail to function, tumors start growing and multiplying uncontrollably. This uncontrolled tumor cell growth interrupts the normal tissue and creates a shear stress on cells eventually killing them. They occupy the cavities within the skull interrupting the normal functions of brain. This elevates the intracranial pressure and damages the nerves of the healthy tissue, not to mention the severe pain that it creates. The tumor may be malignant or benign. World Health Organization (WHO) classified brain tumor into 120 types based on the degree of aggression in behavior, and whether they are primary or secondary tumors. Benign tumors usually grow slowly and are quite localized. Each of these tumors show unique radiographic and biological characteristics when imaged.

A variety of imaging techniques including magnetic resonance imaging (MRI), computed tomography (CT) scans, positron emission tomography (PET) and single photon emission computed tomography (SPECT) scans, and cerebral angiography are used to study brain tumors. CT and MR imaging are preferred in many centers due to their availability, cost-effectiveness as well as their ability to produce high resolution images describing anatomy and pathology. It is

commonly used for brain tumor imaging and has benefits over CT for being: nonionizing, which minimizes the harm to health tissues, highly efficient in terms of generating 3-D images allowing for precise localization of tumors, lower sensitivity to contrast agents, possessing a wider range of soft tissue contrast, and last but not least, capable of acquisition of both functional and anatomical information simultaneously with limited necessity to physically move the patient. Nevertheless, they do not pick up the bones of the skull as well as CT scans and therefore may not show the effects of tumors on the skull.

There are a few reactions to MRI scanning including: panic, nausea, headache, and pain resulting from the injected contrast material.

Several digital image processing and algorithms have been used to view, analyze, and interpret brain images with a goal to make clinically valuable decisions by improving image perception. Texture analysis has been reported since the seventies of last century.

Image texture is commonly defined as function of the spatial variation of pixel intensities in an image. Using three-dimensional (3D) computer graphics applications it generates highly complex and realistic looking surfaces, which provides quantitative information in the form of texture features than cannot be visualized and discriminated by the human eye. The features used during texture analysis are mathematical parameters calculated from the distribution of pixels, which characterize the texture type in the image. The main image processing disciplines in which texture analysis techniques are used are classification, segmentation, and synthesis of dissimilar features including normal tissue, inflammatory regions and tumors.

The number of pixels used define the local features and accordingly classify them into first-order and second order textures. The properties of individual pixel values, are estimated using first-order textures which, in turn use image histograms that include variance; coarseness; skewness; kurtosis; energy; and

entropy. Here, the spatial interaction between the neighboring image pixels. are not taken into account.

Meanwhile, second-order textures estimate properties of several pixel values relative to the neighboring pixels. They are based on calculation of grey tone spatial dependency matrices (GTSDM) elements according to co-occurrence matrix. These include amongst other features: angular second moment, contrast and correlation that can be calculated using different window size.

It was estimated that morality rate was increased up to 300 times as a direct result of brain tumors among developed countries populations with Western and Central Europe had the highest incidence rates, East and South East Asia showed lower incidences. The objective of the imaging modality is to provide clinical finding regarding the tumor existence, size, location, and type. The accurate and prompt diagnosis will usually provide better intervention options for the treatment and increase the survival rate of the patients.

Many researches were published regarding brain tumor diagnosis during various image processing techniques to improve tumor identification and precise location determination. However, the challenge of accurate diagnosis still exists because various tumors have different patterns. Also, it is not easy to discriminate between normal and cancerous tissues at early stage. Therefore, any effort helps the clinician in accurate diagnosis is welcome and it will help in saving lives. The aim was to recognize the brain tumors from the other brain tissues which include: grey and white matter as well as cerebrospinal fluid (CSF). (Buthayna, 2021)

1.1.1 Steps of Image Processing:

The commonly used term "biomedical image processing" means the provision of digital image processing for biomedical sciences. In general, digital image processing covers four major areas (Figure 1.1): Image formation includes all the steps from capturing the image to forming a digital image matrix, Image visualization refers to all types of manipulation of this matrix, resulting in an optimized output of the image, Image analysis includes all the steps of processing, which are used for quantitative measurements as well as abstract interpretations of biomedical images. These steps require a priori knowledge on the nature and content of the images, which must be integrated into the algorithms on a high level of abstraction. Thus, the process of image analysis is very specific, and developed algorithms can be transferred rarely directly into other application domains and Image management sums up all techniques that provide the efficient storage, communication, transmission, archiving, and access (retrieval) of image data. Thus, the methods of telemedicine are also a part of the image management. In contrast to image analysis, which is often also referred to as high-level image processing, low-level processing denotes manual or automatic techniques, which can be realized without a priori knowledge on the specific content of images. This type of algorithms has similar effects regardless of the content of the images. For example, histogram stretching of a radiograph improves the contrast as it does on any holiday photograph. Therefore, low-level processing methods are usually available with programs for image enhancement.

1.2. Problem of the study:

The understanding of the cognitive process of human vision is constantly expanding, much has been learn from the experiment of the visual perception of the image information [(1)]. Tumors is widely used in modern radiotherapy technology. The main issue is the detection of the microscopic tumor cell around its mass; which in general does not change the signal intensity but it can change the textural pattern;

therefore the use of texture analysis technique will make GTV and CTV definition very accurate to be used in treatment of brain tumors and also prevent recurrence.

1.3. Objectives of the Study:

1.3.1 General Objective:

The general objective of this study was to characterize the brain tumors in MRI images (T2 weighted FLAIR) by using of image texture analysis in order to recognize the tumor and its surroundings by its texture feature.

1.3.2 Specific Objectives:

- To identify the region of interest (ROI).
- To classify the extracted feature using k-mean and discriminate analysis.
- To develop classification Map for brain tumors relative to the rest of brain tissue.
- To delineate the radiotherapy GTVs based on selected feature for the brain tumor**.**

1.4. Significance of the Study:

This study highlighted and evaluated the application of texture analysis of brain tumors using image processing programs (IDL) and its techniques, once it need faster and accurate diagnostic modalities in this situation in order to have high diagnostic accuracy in assessing brain tumors and therefore using this scans to plan patient for radiotherapy procedure, which need very accurate delineation of tumor edges in case of CTV and planning target volume in order to deliver sufficient dose to the both volumes and increase therapeutic ratio.

1.5. overview of the study:

This study consisted of five chapters, with chapter one as an introduction; wherein I introduced briefly this thesis and contained (general introduction about image processing in medical imaging, problem of study, general, specific

objectives, and significance and overview of the study). Chapter two was literature review about textural analysis in the case of brain MRI using different image processing techniques. Chapter three described the methodology (material, method) that were used to achieve the thesis result. Chapter four included presentation (result) of final study; chapter five was discussion, conclusions and recommendations for future scope in addition to references and appendices.

Chapter Two
2. Literature review

Chapter Two
2. Literature review

2.1. Image Processing Technique:

In addition to originally digital methods, such as Computed Tomography (CT) or Magnetic Resonance Imaging (MRI), initially analogue imaging modalities such as endoscopy or radiography are nowadays equipped with digital sensors. Digital images are composed of individual pixels, to which discrete brightness or color values are assigned. They can be efficiently processed, objectively evaluated, and made available at many places at the same time by means of appropriate communication networks and protocols, such as Picture Archiving and Communication Systems (PACS) and the Digital Imaging and Communications in Medicine (DICOM) protocol, respectively. Based on digital imaging techniques, the entire spectrum of digital image processing is now applicable in medicine.

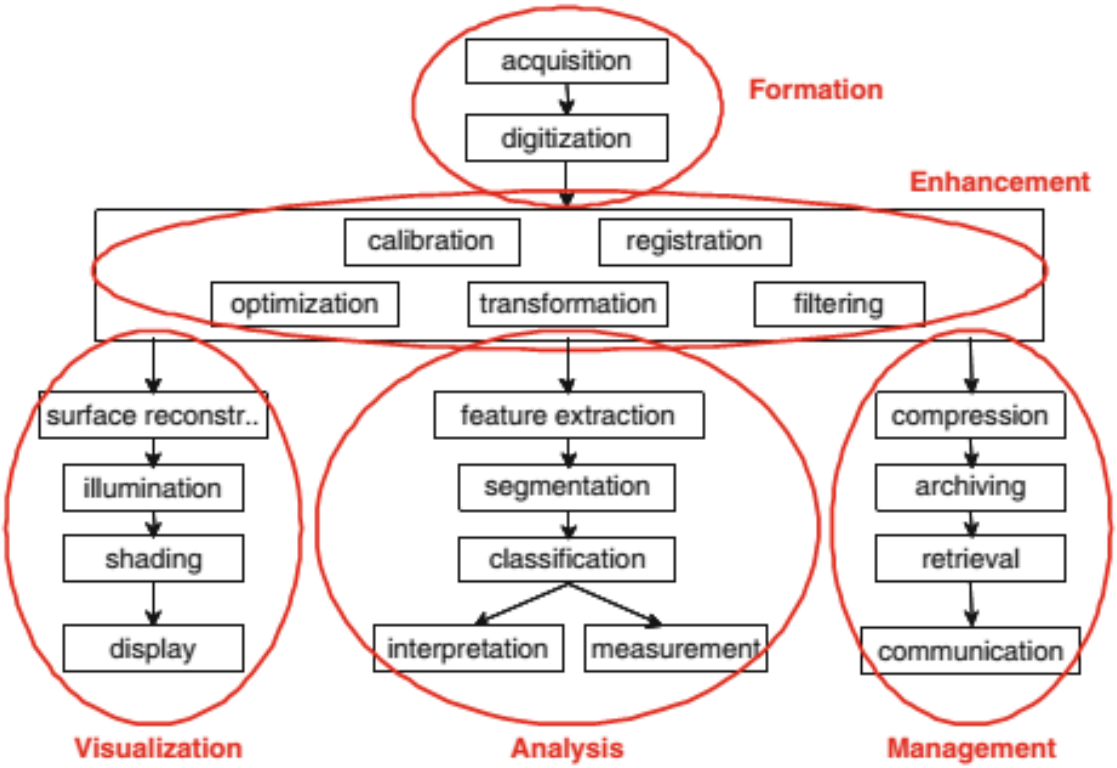

Fig. (2.1) Modules of image processing.

The commonly used term “biomedical image processing” means the provision of digital image processing for biomedical sciences. In general, digital image processing covers four major areas (Figure 1.1): Image formation includes all the steps from capturing the image to forming a digital image matrix, Image visualization refers to all types of manipulation of this matrix, resulting in an optimized output of the image, Image analysis includes all the steps of processing, which are used for quantitative measurements as well as abstract interpretations of biomedical images. These steps require a priori knowledge on the nature and content of the images, which must be integrated into the algorithms on a high level of abstraction. Thus, the process of image analysis is very specific, and developed algorithms can be transferred rarely directly into other application domains and Image management sums up all techniques that provide the efficient storage, communication, transmission, archiving, and access (retrieval) of image data. Thus, the methods of telemedicine are also a part of the image management. In contrast to image analysis, which is often also referred to as high-level image processing, low-level processing denotes manual or automatic techniques, which can be realized without a priori knowledge on the specific content of images. This type of algorithms has similar effects regardless of the content of the images. For example, histogram stretching of a radiograph improves the contrast as it does on any holiday photograph. Therefore, low-level processing methods are usually available with programs for image enhancement.

2.2. brain tumors:

Primary tumors of the central nervous system (CNS) are relatively uncommon, accounting for only 2% of cancer deaths. However, the effect on the individual with a primary CNS tumor is frequently devastating, and brain tumors lead, on average, to a greater loss of life per patient than any other adult tumor. Primary CNS tumors affect patients of all ages, from childhood to old age, with a rising incidence from middle age onwards. In childhood, they are the commonest solid tumors (as opposed to leukaemias). The overall annual incidence is around 7 per

100 000 populations, giving approximately 4400 people newly diagnosed with a brain tumor in the UK each year (H. Symonds et al 1994).

An incidence of the brain tumors according to its tissue type as; adult primary CNS tumors: 30–35% meningioma, 20% GBM, 10% pituitary, 10% nerve sheath, 5% low-grade glioma, <5% anaplastic astrocytoma, <5% primary CNS lymphoma. Of adult gliomas, ~80% are high-grade and ~20% are low-grade. Children: 20% of all pediatric tumors (second to ALL). Twenty percent JPA, 15–20% malignant glioma/GBM, 15% medulloblastoma, 5–10% pituitary, 5–10% Ependymoma, <5% optic nerve glioma. Possible etiologic associations: rubber compounds, polyvinyl chloride, N-nitroso compounds, and polycyclic hydrocarbons. Prior ionizing RT has been associated with new meningiomas, gliomas, and sarcomas (~2% at 20-year), [3]. There is a huge range in outcome for patients with primary CNS tumors, from almost guaranteed cure in some conditions (e.g. germinoma) to almost guaranteed fatality in others (e.g. glioblastoma (GBM)) (C.D Kubicky et al 2010).

2.2.1. MRI brain imaging and characteristics of brain tumors:

there is a variety of imaging techniques used to study brain tumors such as: MRI, CT, PET, SPECT and cerebral angiography. In recent years, CT and MR imaging are the most widely used techniques, because of their widespread availability and their ability to produce high resolution images of normal anatomical structures and pathological tissues. MRI is a method used to visual physiological and pathological alterations of living tissues and is commonly used for brain tumor imaging because of the following reasons: (Medical Imaging in Cancer Care 2012) it does not use ionizing radiation like CT, SPECT and PET. Its contrast resolution is higher than other techniques mentioned above. Ability of MRI devices to generated three dimensional space images enables them to have superior tumor location. Its ability in acquisition of both functional and anatomical information about the tumor during the same scan.

2.3. Texture Analysis

Image texture, defined as a function of the spatial variation in pixel intensities (gray values), is useful in a variety of applications and has been a subject of intense study by many researchers. Texture is the most important visual clue in identifying the types of homogeneous regions. This is called texture classification. The goal of texture classification then is to produce a classification map of the input image where each uniform textured region is identified with the

texture class it belongs to. We could also find the texture boundaries even if we could not classify these textured surfaces. This is then the second type of problem that texture analysis research attempts to solve texture segmentation. The goal of texture segmentation is to obtain the boundary map. Texture synthesis is often used for image compression applications. It is also important in computer graphics where the goal is to render object surfaces which are as realistic looking as possible. The goal is to extract three-dimensional shape information from various cues such as shading, stereo, and texture. The texture features (texture elements) are distorted due to the imaging process and the perspective projection which provide information about surface orientation and shape (H.C Chen et al 1998)**.**

2.3.1. Medical Image Texture Analysis :

Image analysis techniques have played an important role in several medical applications. In general, the applications involve the automatic extraction of features from the image which is then used for a variety of classification tasks, such as distinguishing normal tissue from abnormal tissue. Depending upon the particular classification task, the extracted features capture morphological properties, color properties, or certain textural properties of the image. The textural properties computed are closely related to the application domain to be used for example Harms et.al **(**H. Harms et al 1986**)** used image texture in combination with color features to diagnose leukemic malignancy in samples of stained blood cells. They extracted texture micro-edges and "textons" between these micro-edges. The textons were regions with almost uniform color. They extracted a number of texture features from the textons including the total number of pixels in the textons which have a specific color, the mean text on radius and text on size for each color and various text on shape features. In combination with color, the texture features significantly improved the correct classification rate of blood cell types compared to using only color features. (Landeweerd and Gelsema 1978) extracted various first-order statistics (such as mean gray-level in a region) as well as second-order statistics (such as gray level co-occurrence matrices) to differentiate different types of white blood cells. (Insana et.al1986**)** used textural features in ultrasound images to estimate tissue scattering parameters. They made significant use of the knowledge about the physics of the ultrasound imaging process and tissue characteristics to design the texture model (H.C Chen et al 1998)**.**

2.3.2. Statistical Approaches for Texture Analysis:

Texture analysis is presented here as a useful computational method for discriminating between pathologically different regions on medical images because it has been proven to perform better than human eyesight at discriminating certain classes of texture. In first-order statistical texture analysis, information on texture is extracted from the histogram of image intensity. This approach measures the frequency of a particular grey-level at a random image position and does not take into account correlations, or co-occurrences, between pixels. In second-order statistical texture analysis, information on texture is based on the probability of finding a pair of grey-levels at random distances and orientations over an entire image. Extension to higher-order statistics involves increasing the number of variables studied (W. Nailon 2010).

First-Order Statistical Texture Analysis: First-order texture analysis measures use the image histogram, or pixel occurrence probability, to calculate texture. The main advantage of this approach is its simplicity through the use of standard descriptors (e.g. mean and variance) to characterize the data (J.K. Keller et al 1989)**.** However, the power of the approach for discriminating between unique textures is limited in certain applications because the method does not consider the spatial relationship, and correlation, between pixels. For any surface, or image, grey-levels are in the range where N_g is the total number of distinct grey-levels, If (N_i) is the number of pixels within $o \leq i \leq N_8 - 1$ intensity i and M is the total number of pixels in an image, it follows that the histogram, or pixel occurrence probability, is given by

$$P(i) = \frac{N(i)}{M}$$

In general seven features commonly used to describe the properties of the image histogram, and therefore image texture, are computed. These are: mean; variance; coarseness; skewness; kurtosis; energy; and entropy (W. Nailon 2010).

Second-Order Statistical Texture Analysis: The human visual system cannot discriminate between texture pairs with matching second order statistics. The first machine-vision framework for calculating second-order or pixel co-occurrence texture information was developed for analyzing aerial photography images (R.M. Haralick 1993). In this technique pixel co-occurrence matrices, which are commonly referred to as grey-tone spatial dependence matrices (GTSDM), are computed. The entries in a GTSDM are the probability of finding a pixel with grey-level i at a distance d and angle α from a pixel with a grey-level j. This may be written more formally as P(I,j:d,α). An essential component of this framework

is that each pixel has eight nearest-neighbors connected to it, except at the periphery. As a result four GTSDMs are required to describe the texture content in the horizontal ($P_H=0^0$), vertical ($P_V=90^0$), right- ($P_{RD}=45^0$), and left-diagonal ($P_{LD}=135^0$).

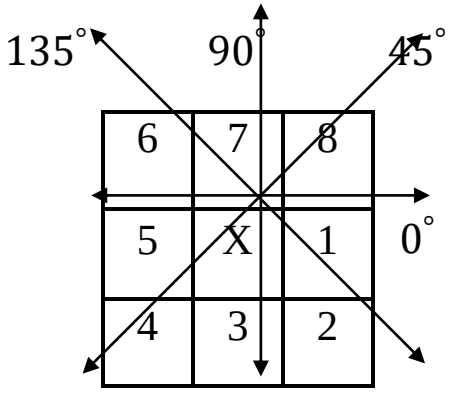

Fig.2.3. Eight nearest-neighbor pixels used in the GTSDM framework to describe pixel connectivity. Cells 1 and 5 show the horizontal (P_H) 4 and 8 the right-diagonal (P_{RD}), 3 and 7 the vertical (P_V), and 2 and 6 the left-diagonal (P_{LD}) nearest-neighbors.

An example of the calculation of a horizontal co-occurrence matrix (P_H) on a 4×4 image containing four unique grey-levels is shown in Fig. 2.4. A complete representation of image texture is contained in the co-occurrence matrices calculated in the four directions.

Extracting information from these matrices using textural features, which are sensitive to specific elements of texture, provides unique information on the structure of the texture being investigated. Haralick et al. (R.M. Haralick 1993) proposed a set of 14 local features specifically designed for this purpose. In practice the information provided by certain features may be highly correlated or of limited practical use. A feature selection strategy is therefore useful with this approach to take account of redundant, or irrelevant, information.

It is also interesting to note that prior to any processing the GTSDMs, which are symmetric, can provide some useful information on the characteristics of the image being studied. For example, the co-occurrence matrix entries for a coarse texture will be heavily focused along the diagonals relative to the distance d between the pixels studied.

0	2	2	2
0	3	2	2
1	2	2	2
3	0	3	0

(P_H)

Grey-Level				
Grey-Level	0^0	0	1	2	3
0	0	0	1	4
1	0	0	1	0
2	1	1	10	1
3	4	0	1	0

Fig.2.4. Simple example demonstrating the formation of a co-occurrence matrix from an image. Left, 4*4 image with four unique grey-levels. Right, the resulting horizontal co-occurrence matrix (P_H).

Angular second moment

Contrast, $$f_1 = \sum_{i=1}^{N_q}\sum_{i=1}^{N_q} \acute{p}\,(i,j)^2$$

$$f_2 = \sum_{i=0}^{N_q-1} n^2 \left[\sum_{i=1}^{N_q}\sum_{i=1}^{N_q} \acute{p}\,(i,j)\right]_{i-j=n}$$

Correlation,

$$f_3 = \sum_{i=1}^{N_q}\sum_{i=1}^{N_q} \frac{(i-\mu_x)\big(j-\mu_y\big)\acute{p}(i,j)}{\sigma_x\,\sigma_y},$$

where, N_q is the number of distinct grey-levels in the input and, μ_x, μ_y, σ_x, are the means and standard deviations of P(i,j). Throughout, $P(i,j) = \frac{P(i,j)}{R}$ where P(i,j) is (P_H,P_V,P_{LD},P_{RD}) and R is the maximum number of resolution cells in a GTSDM (W. Nailon 2010).

Higher-Order Statistical Texture Analysis: The grey-level run length method (GLRLM) is based on the analysis of higher-order statistical information. In this approach GLRLMs contain information on the run of a particular grey-level, or grey-level range, in a particular direction. The number of pixels contained within the run is the run-length.

A coarse texture will therefore be dominated by relatively long runs whereas a fine texture will be populated by much shorter runs. The number of runs (r) with gray-level (i), or lying within a grey-level range (I), of run length j in a direction α is denoted by $R(\alpha) = \left\{\frac{r(I,j)}{\alpha}\right\}$.

This is analogous to the GTSDM technique (A.K. Jain and B. Chandrackaran 1982) as four GTRLMs are commonly used to describe texture runs in the directions ($0^{0,}$ $90^{0,}$ 180^{0} AND 135^{0}). on linearly adjacent pixels. An example of the calculation of a horizontal GLRLM is shown in Fig. 2.10.

0	1	2	2
0	3	2	2
1	2	2	2
3	0	3	0

Grey-Level \ Run-Length	0^0	1	2	3	4
	0	4	0	0	0
	1	2	0	0	0
	2	0	2	1	0
	3	3	0	0	0

Fig. 2.5 Simple example demonstrating the formation of a GLRLM. Left, 4*4 image with four unique grey-levels. Right, the resulting GLRLM in the direction 0^0.

A set of seven numerical texture measures are computed from the GTRLMs. Three of these measures are presented here to illustrate the computation of feature information using this framework.

Short Run Emphasis,

$$f_{SR} = \frac{1}{T_R} \sum_{i=0}^{N_g-1} \sum_{J=1}^{N_r} \frac{\acute{r}(i,j|\alpha)}{j^2},$$

Long Run Emphasis,

$$f_{LR} = \frac{1}{T_R} \sum_{i=0}^{N_g-1} \sum_{j=1}^{N_r} j^2 \, \acute{r}(i,j|\alpha),$$

Grey-Level Distribution,

$$f_{GD} = \frac{1}{T_R} \sum_{i=0}^{N_g-1} \left[\sum_{j=1}^{N_r} \acute{r}(i,j|\alpha) \right]^2,$$

Where Ng is the maximum number of grey-levels, Nr is the number of different run lengths in the matrix and,

$$T_R = \sum_{i=0}^{N_g-1} \sum_{j=1}^{N_r} \acute{r}(i,j|\alpha),$$

T_R serves as a normalizing factor in each of the run length equations (W. Nailon 2010).

2.3.3. Feature Selection, Reduction and Classification:

The texture analysis approaches presented in the preceding sections calculate features that describe properties of the image, or region, being studied. This information is next used in a pattern recognition system to classify the objects, or texture patterns of interest, into an appropriate number of categories or classes (W. Therrien et al 1989)**.** However, some of the features calculated may be highly correlated and some may contain irrelevant information. Feature selection is used to select a subset of features p $\boldsymbol{s}$ from a given set of $\boldsymbol{p}$ features such that $\boldsymbol{S}p \leq \boldsymbol{p}$ and there is no significant degradation in the performance of the classification system (W. Therrien et al 1989); and (A.K. Jain and B. Chandrackaran 1982), The reduction of the feature set reduces the dimensionality of the classification problem and in some cases can increase the performance of the classification accuracy due to finite sample size effects (P.A. Devijver and J. Kittler 2012). Two powerful methods for reducing the number of features are presented. These are the sequential forward search (SFS) algorithm and its backward counterpart the sequential backward search (SBS) algorithm (J. Nouza 1995)**.** Pattern recognition system must also be capable of partitioning, or clustering, the reduced feature set into classes of similar observations. The *K*-means algorithm belongs to the collection of multivariate methods used for classifying, or clustering, data and is presented because of its general applicability in classification problems (W. Therrien et al 1989)**.**

2.3.4. Feature Selection Using the Sequential Forward Search Algorithm

The SFS algorithm is a bottom-up strategy for removing redundant or irrelevant features from the feature matrix (J. Nouza 1995). At each successive iteration the feature that produces the largest value of the selection criterion function *J* is added to the current feature set. Given a set of candidate features $Y \in \boldsymbol{R}$, a subset $X \in \boldsymbol{R}$ is selected without significant degradation to the classification system (A.K. Jain and B. Chandrackaran 1982). The best subset *X*,

$$\boldsymbol{X} = \{\boldsymbol{x_i}|\boldsymbol{i} = \boldsymbol{1}, \boldsymbol{2}, \dots, \boldsymbol{d}, \quad \boldsymbol{x_i} = \boldsymbol{\gamma}\}, \qquad (\mathbf{16})$$

Of *d* features where $(d \leq D)$ is selected from the set,

$$\boldsymbol{\gamma} = \{\boldsymbol{y_1}|\boldsymbol{j} = \boldsymbol{1}, \boldsymbol{2}, \dots, \boldsymbol{D}\}, \qquad (\mathbf{17})$$

By optimizing the criterion function *J*, chosen here to be the estimated minimum probability of error. For the set of measurements taken from *Y*, ideally the probability of correct classification (ל), with respect to any other combination, is given by,

$$\boldsymbol{\Xi} = \{\xi_i|i = 1,2, \dots., d\} \qquad (18)$$

It follows that the minimum probability of error for the space spanned by ξ, for each class ω_i id defined as,

$$\boldsymbol{E}(\boldsymbol{\Xi}) = \int \left[1 - \max\left(P(\omega_i|\xi)\right)\right] p(\xi) d(\xi), \quad (19)$$

And the desired criterion function,

$$J(X) = \min(E(\boldsymbol{\Xi})) \qquad (20)$$

One of the disadvantages of the SFS approach is that it may suffer from nesting. That is, because features selected and included in the feature subset cannot be removed, already selected features determine the course of the remaining selection process. This has noticeable hazards since after further iterations a feature may become superfluous. Another limitation of the SFS approach is that in the case of two feature variables, which alone provide little discrimination but together are very effective, the SFS approach may never detect this combination. To overcome this problem it is useful to start with a full set of available features and eliminate them one at a time. This is the method adopted by the SBS approach (W. Nailon 2010).

2.3.5. Feature Selection Using the Sequential Backward Search Algorithm:

The SBS is a top down approach, which starts with the complete feature set and removes one feature at each successive iteration (J. Nouza 1995). The feature that is chosen to be removed is the feature that results in the smallest reduction in the value of the selection criterion function when it is removed. In general, the SBS algorithm requires more computation than the SFS algorithm because initially it considers the number of features in the complete set as forming the subset. Although the SBS overcomes some of the difficulties of the SFS approach the resulting feature subset is not guaranteed to be optimal. Furthermore, like its counterpart the SBS algorithm suffers from nesting because once a feature is selected it cannot be disregarded. Implementation of the SBS approach is analogous to the SFS approach detailed in SFS section. The SBS algorithm is computationally more expensive than the SFS algorithm, however, their performance is comparable. Despite the shortcomings of the SFS and SBS techniques they are powerful techniques for reducing the feature set of real-world pattern recognition problems (J.A. Hartigan 1975).

2.3.6. Classification Using the *K*-means Algorithm:

The general clustering problem is one of identifying clusters, or classes, of similar points. For the specific problem presented in this chapter this would involve clustering the features calculated on a specific image region into a unique cluster. The number of classes may be known or unknown depending on the particular problem. The *K*-means algorithm belongs to the collection of multivariate methods used for clustering data (W. Therrien et al 1989); **(**J.L. Duda et al 2001**)** and (P.T. Meyer et al 2017). The algorithm starts with a partition of the observations into clusters. At each step the algorithm moves a case from one cluster to another if the move will increase the overall similarity within clusters. The algorithm ceases when the similarity within clusters can no longer be increased. Assuming that the number of clusters *c N* is known in advance the *K*-means technique may be defined by the following three stages. Assuming that the number of clusters *c N* is known in advance the *K*-means technique may be defined by the following three stages.

Stage 1 – Initialization: For the set of observations $\{Y = y_1, y_2, \dots \dots . y_N\}$ to be classified into the set of classes $\Omega = \{W_1, W_2, \dots \dots . W_n\}$, the algorithm starts with an arbitrary partition of the observations into *Nc* clusters and computes the mean vector of each cluster (μ_1, μ_2, μ_{Nc}) using the Euclidean distance $\|y_i - \mu_k\|^2$where μ_k is the sample mean of the *kth* cluster.

Stage 2 - Nearest Mean: Assign each observation in ***Y*** to the cluster with the closest mean.

Stage 3 - Update and Repeat: Update the mean vector for each cluster and repeat *Stage 2* until the result produces no significant change in the cluster means.

2.3.7. Texture Analysis of Radiotherapy Planning Target Volumes:

Case study based information*:* In the first, a texture analysis approach was used to classify regions of distinct pathology on CT images acquired on eight bladder cancer patients. In the second, texture analysis was used to study the distribution of abnormal prion protein found in the molecular layer of the cerebellum of cases of vCJD and sporadic CJD. The goal of radiotherapy, the treatment of cancer with ionizing radiation, is to deliver as high a dose of radiation as possible to diseased tissue whilst sparing healthy tissue. In curative (radical) radiotherapy planning, delineation of the gross tumor volume (GTV) is primarily based on visual assessment of CT images by a radiation oncologist (M.L. Welton et al 2001). The accuracy therefore of the GTV is dependent upon the ability to visualize the tumor and as a result significant inter- and intra-clinician variability has been reported in the contouring of tumors of the prostate, lung, brain and esophagus **(**R. Steenbakkers et al 2005**)** and (B.B. Mandelbrot 1977).

The aim of the work presented in this case study was to develop a texture analysis methodology capable of distinguishing between the distinct pathology of the GTV and other clinically relevant regions on CT image data. For eight bladder patients (six male and two female), CT images were acquired at the radiotherapy planning stage and thereafter at regular intervals during treatment. All CT scans were acquired on a General Electric single slice CT scanner (IGE HiSpeed Fx/I, GE Medical Systems, Milwaukee, WI, USA). Seven patients were scanned with a 3 mm slice thickness and one patient with a 5 mm slice thickness. The repeat CT scans were registered against the corresponding planning reference CT scan to allow comparison of the same region on each image. Image features based on: the first-order histogram (N=7); second-order GTSDM (N=14); higher-order GLRLM(N=5); and a bespoke box-counting fractal approach (N=1) were calculated on preidentified regions of the CT images of each patient (W. Nailon 2010). Two classification environments were used to assess the performance of the approach in classifying the bladder, rectum and a region of multiple pathology on the axial, coronal and sagittal CT image planes. These were, in the first using all of the available features (N=27) and in the second using the best three features identified by the SFS approach. The classification results achieved are presented in Fig. 11. No significant discrimination was observed between the bladder,

rectum and the region of multiple pathology on the axial, coronal and sagittal CT data using all of the available features (N=27). On the contrary, using the three best features identified by the SFS feature reduction approach, significant discrimination between the three pathological groups was possible. These results demonstrate the significant improvement in classification that can be achieved by removing features with little discriminatory power. Moreover the results demonstrate the effectiveness of texture analysis for classifying regions of interest, which may be difficult for the human observer to interpret. The features that were found to work best were all from the GTSDM approach. The feature produced by the bespoke box-counting fractal approach was not found to have significant discriminatory power. However, more research is required into the use of fractal methods in this application area, particularly because assigning a single dimension to a whole region may not be appropriate (L. Hassan et al 2016).
Furthermore, the fractal dimension calculation may have been influenced by the different distribution of grey-levels in the images due to variations in the amount of urine in the bladder and air in the rectum[10] .

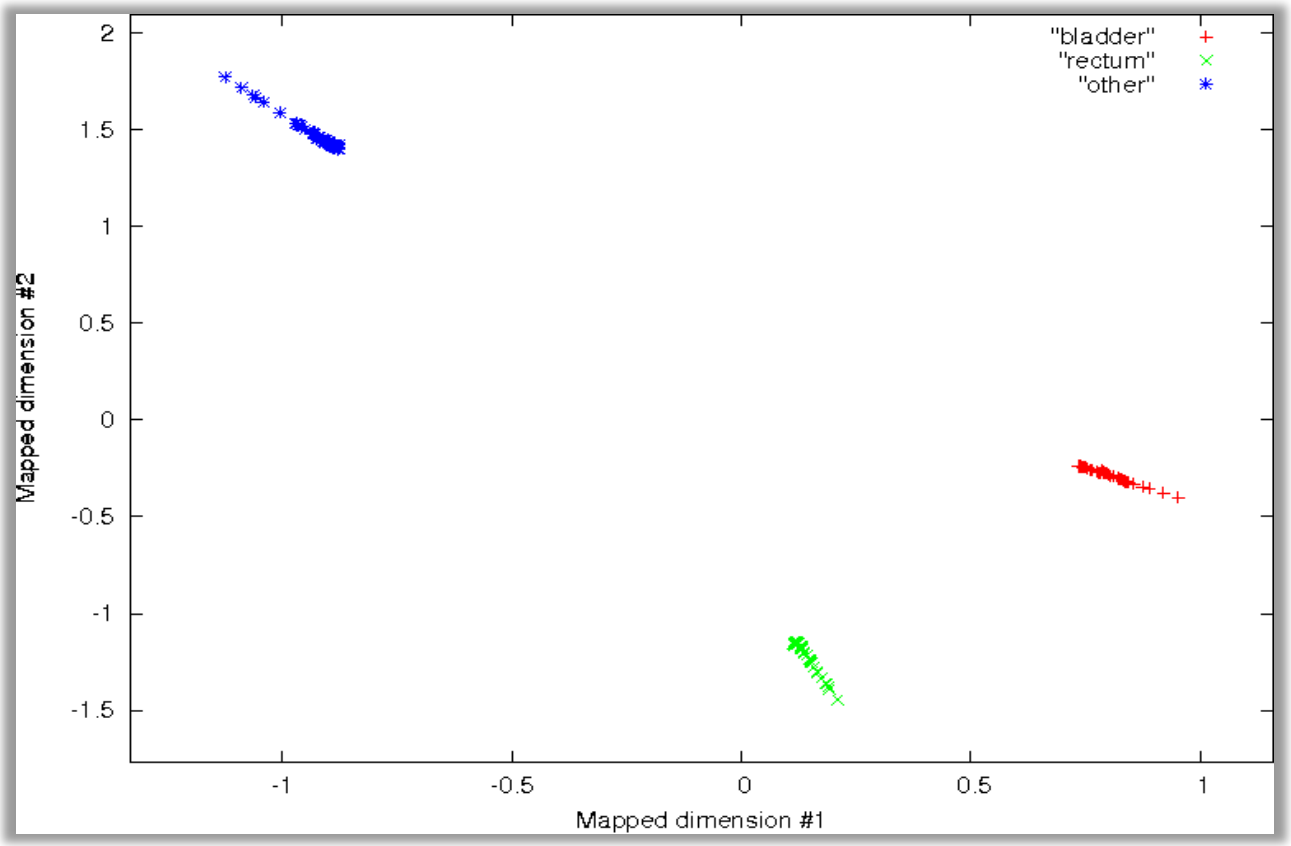

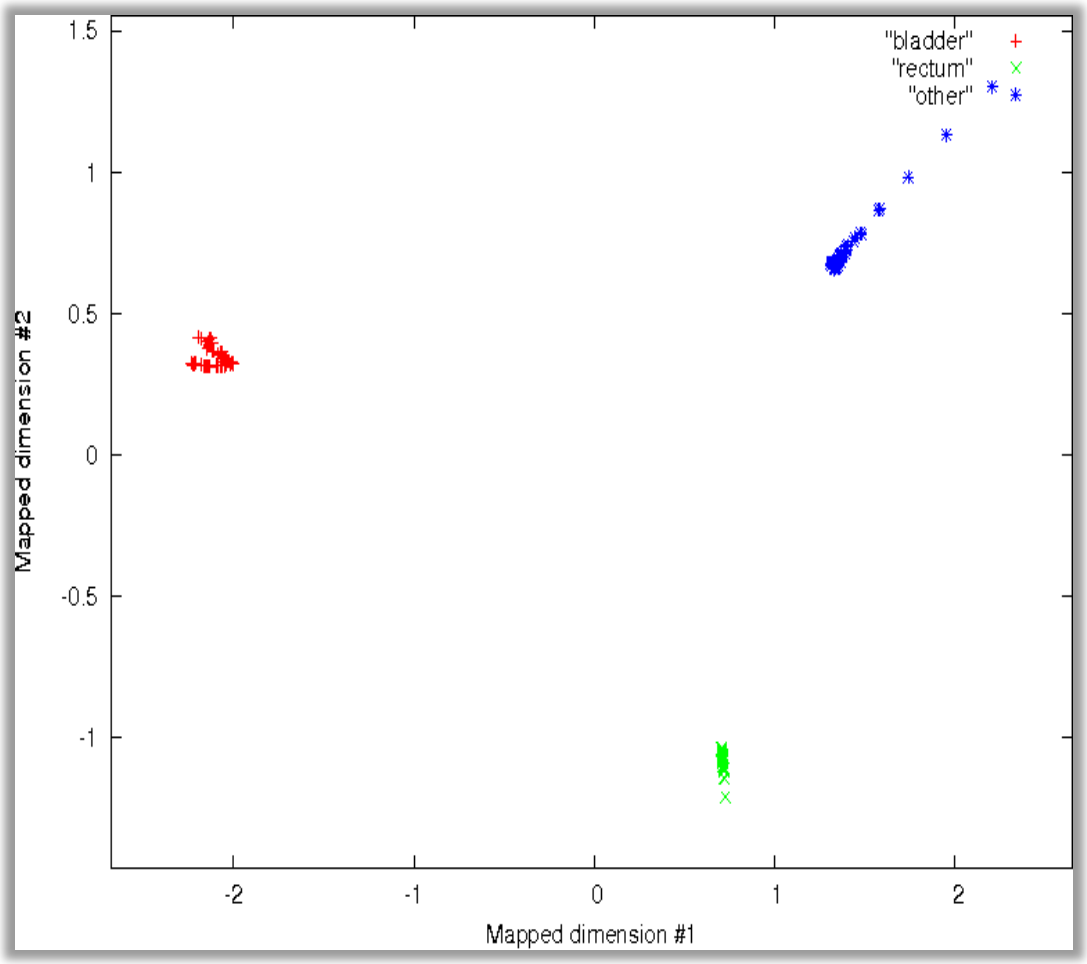
"bladder"
"rectum"
"other"
Mapped dimension #2
Mapped dimension #1
1.5
1
0.5
0
-0.5
-1
-2
-1
0
1
2

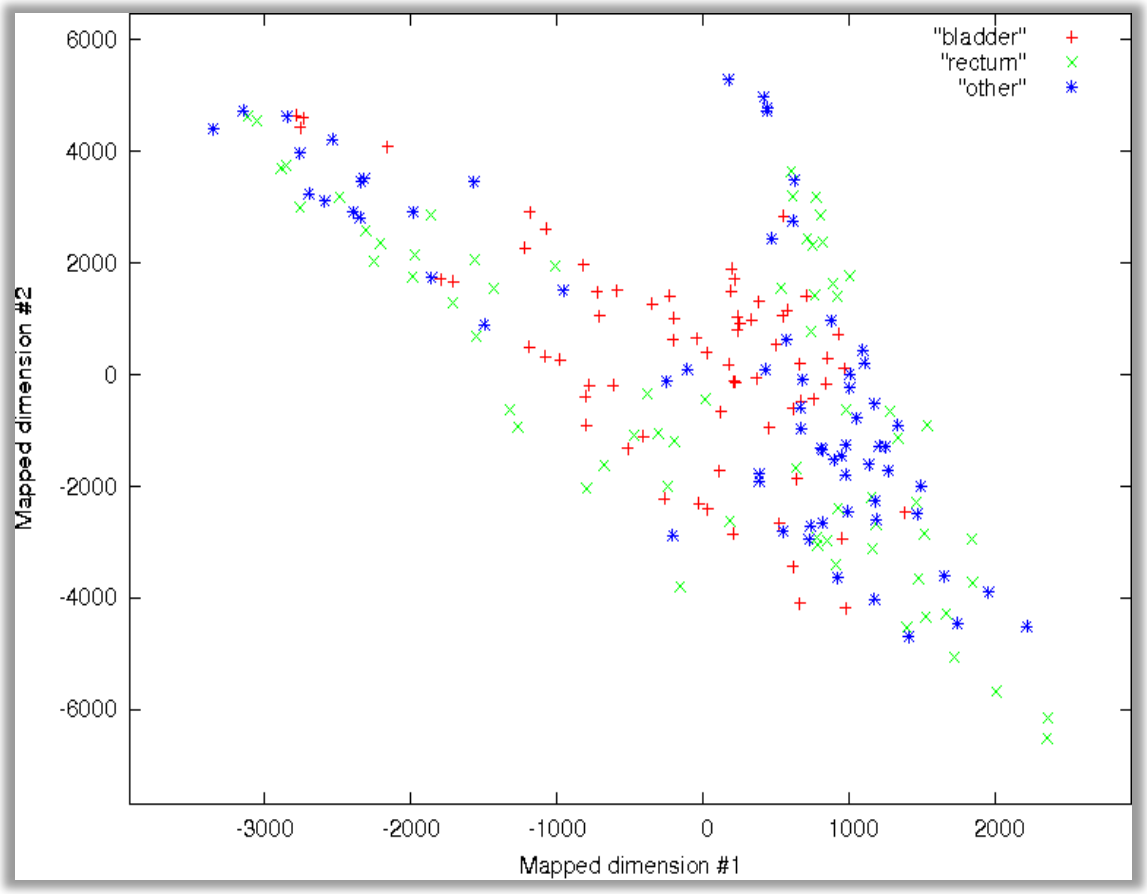
"bladder"
"rectum"
"other"
Mapped dimension #2
Mapped dimension #1
6000
4000
2000
0
-2000
-4000
-6000
-3000
-2000
-1000
0
1000
2000

Fig. 2.6 Classification of the bladder, rectum and a region of multiple pathology identified as other on axial CT images through the pelvis using a texture analysis approach. Left (top: axial, middle: coronal, bottom: sagittal) plots showing the result of using all available features to classify the bladder, rectum and other. Right (top: axial, middle: coronal, bottom: sagittal) plots showing classification of the bladder, rectum and other using the best three features identified by the SFS approach.

The approach was also found to be insensitive to CT resolution and slice thickness for the data set studied. It was also noticed that discrimination of the bladder, rectum and other region in the coronal and sagittal image planes was comparable to the discrimination obtained in the axial plane. This is encouraging given that the coronal and sagittal data sets were produced from the axial data and suffer a loss of resolution because of finite CT slice thickness in the axial data acquisition procedure.

2.8. Previous Study

A. A. B. Hassan et.al (2016) [(24)] aimed to characterize brain glioma in magnetic resonance images using image texture analysis techniques in order to recognize the tumor and surrounding tissues by means of textural features. This is an analytical case control study was conducted in radiation oncology department at radiation and isotopes center of Khartoum (RICK), which included 100 patients underwent MRI for brain (50 with brain glioma and the rest with normal scan), FLAIR, T2, T1, and T1 with contrast sequence was performed then the image extracted as DICOM images and then converted to TIFF format which used as input data for an algorithm generated using IDL (interactive data language) for textural features extraction. Three basic textural features types was used to classify the brain images using five different window sizes (3x3, 5x5, 10x10, 15x15, and 20x20 pixels) which are first order statistics (FOS), second order statistics, and diagonal features, to recognizes 4 different classes (brain gray and white matter, tumor, background and CSF); further analysis and image segmentations was performed to remove background from the images for purpose of image enhancement. The extracted feature classified using linear discriminant analysis. The result showed that the classification accuracy, sensitivity and specificity according to window sizes was (99.5%, 98.4% and 100%), (98.5%, 95.7% and 100%), (99.1%, 98.8% and 99.3%), (98.1%, 94.3% and 100%), and (96.1%, 90.0% and 98.8%) respectively for brain glioma. This study implies that 3x3 window gives a higher classification accuracy while the most significant

features for classification includes; difference average of SGLD, mean and entropy of FOS.

Hammad et.al (2008) [25] aimed to propose a combined approach for meningioma subtype classification using sub band texture (macro) features and micro-texture features. These are captured using the Adaptive Wavelet Packet Transform (ADWPT) and Local Binary Patterns (LBPs), respectively. These two different textural features are combined together and used for classification. The effect of various dimensionality reduction techniques on classification performance is also investigated. We show that high classification accuracies can be achieved using ADWPT. Although LBP features do not provide higher overall classification accuracies than ADWPT, it manages to provide higher accuracy for a meningioma subtype that is difficult to classify otherwise

Pantelis Georgia et.al (2009) [26] aimed to evaluate the efficiency of 3D textural features using a pattern recognition system in the task of discriminating benign, malignant and metastatic brain tissues on T1 post contrast MR imaging (MRI) series. The dataset consisted of 67 brain MRI series obtained from patients with verified and untreated intracranial tumors. The pattern recognition system was designed as an ensemble classification scheme employing a support vector machine classifier, specially modified in order to integrate the least squares features transformation logic in its kernel function. The latter, in conjunction with using 3D textural features, enabled boosting up the performance of the system in discriminating metastatic, malignant and benign brain tumors with 77.14%, 89.19% and 93.33% accuracy, respectively. The method was evaluated using an external cross-validation process; thus, results might be considered indicative of the generalization performance of the system to "unseen" cases. The proposed system might be used as an assisting tool for brain tumor characterization on volumetric MRI series.

Solomou et.al (2008)[27] aimed to investigate the efficiency of the combination of textural MRI features and MRS metabolite ratios by means of a pattern recognition system in the task of discriminating between meningiomas and metastatic brain tumors. The data set consisted of 40 brain MR image series and their corresponding spectral data obtained from patients with verified tumors. The pattern recognition system was designed employing the support vector machines classifier with radial basis function kernel; the system was evaluated using an external cross validation process to render results indicative of the generalization performance to "unknown" cases. The combination of MR textural and

spectroscopic features resulted in 92.15% overall accuracy in discriminating meningiomas from metastatic brain tumors. The fusion of the information derived from MRI and MRS data might be helpful in providing clinicians a useful second opinion tool for accurate characterization of brain tumors.

Chapter Three

3. Materials and Methods

Chapter Three

3. Materials and Methods

This study aimed to characterize the brain tumors in magnetic resonance images using image texture analysis, the data were collected form Antalya Diagnostic Center, from 50 database image (five patient diagnosed with brain tumors underwent MR examination of brain)

3.1. Material:

The study executed using magnetic resonance imaging scanner; Signa HDxt 1.5T provides with advanced technology, such as: A proven, homogeneous 1.5T magnet delivering a full 48cm field of view. 16-channel RF. HD gradients engineered for high-fidelity to produce high accuracy waveforms. HD Reconstruction engineered for real-time, high-performance image generation. Advanced, high-definition applications such as Cube and IDEAL that help deliver images with premium quality and clarity.

High-Density coils engineered with coil elements that are optimized for the anatomy and exam. GE Signa HDx 1.5T Technical Specifications**;** magnet: 1.5 Tesla, Superconducting, Clinical Application: Whole Body, Configuration: Compact Short Bore, Power Requirements: 480 or 380/415, Cooling System: Closed-loop water-cooled gradient, Cryogen Use: Less than 0.03 L/hr liquid helium, Spectroscopy: Possible, Synchronization: ECG/peripheral, respiratory gating, (SmartPrep, SmartStep), Pulse Sequences (Standard): SE, IR, 2D/3D GRE and SPGR, Angiography: 2D/3D TOF, 2D/3D Phase Contrast; 2D/3D FSE, 2D/3D FGRE and FSPGR, SSFP, FLAIR, EPI, Pulse Sequences (Optional): 2D/3D Fiesta, FGRET, Spiral, Tensor , imaging Modes: 2D single slice, multi slice, and 3D volume images, multi slab, cine, FOV: 1cm to 48cm continuous, Slice Thickness: 2D 0.7mm to 20mm; 3D 0.1mm to 5mm, Display Matrix: 1028 x 1024, Measuring Matrix: 128 x 512 steps 32 phase encode and Pixel Intensity 256 gray levels.

3.2. Methods :

Technique: The patient under examination must perform MRI brain the technique performed to scan lesion; Axial T1 - orT2-W FLAIR. The vast majority of intracranial lesions exhibit long T2 values. FLAIR is a similar sequence to STIR but in this case it uses a longer inversion time (approximately 2200ms) to suppress CSF and increase conspicuity of the lesion. The axial plane is useful as it is comparable to CT (TE/TR/TI = 148 /9200ms /2200ms FOV = 22–25cm, Slice thickness/gap = 5/1mm). where the tumor appears to have relatively hypo intense area surround with hyper intense area due to pre-tumoral edema surround brain mass in case of T2 weighted images, also the flair axial T2, axial T1, coronal T2 and T1 AXIAL and sagital with gadolinium contrast was done to assess the lesion and its surrounding structure and the multifoculity of the tumors if existed. starting from the both with contrast images and without contrast images was used to determine tumor site and size and tumor relations was assessed using network and computer PACS system was used to visualize the images and patient diagnosis was extracted.

Then the images prepared for the textural analysis throw DICOM viewer to select which images can be treated as IDL variable and then the processing can be achieved for classification purposes.

3.2.1 Method of data collection:

The images that collected from the PACS viewed using RadiAnt DICOM Viewer software, the classification was aimed to extract the feature from the image based on the normal image histogram where the primary image was converted into tiff format as an input image for IDL image processing program. Then the images were read by IDL in JEPG format and then clicked on areas represents the brain tumor, normal brain tissue, CSF and fatty tissue. The pixel intensity in these areas was assigned as classification center, and then the image classified into one of these classes then a window of 3x3 was created in order to scan the image then the feature were extracted for the; mean; variance;

coarseness; skewness; kurtosis; energy; and entropy. All these feature were calculated for all images and then the data were ready for discrimination which was performed using step-wise technique in order to select the most significant feature that can be used to classify the brain tumor in MR imaging. Then the classification map were further processed by region label to segment the brain tissue from the rest of the structure and convert the segmented the brain tissue from the classification map to binary image to extract the brain tumor from the whole original image.

3.2.2 Study design:

This is an analytical study where the samples were selected randomly.

3.2.3 Study area:

This study conducted in Antalia Medical center, Khartoum state / Sudan

3.2.4 Sampling:

A database of 50 images 5 (Images from axial T2 and T2 weighted MR image with contrast from five patients was gathered), selected randomly, the study include patients diagnosed with brain tumors in both gender and all age.

3.2.5 Study Duration

This study conducted in period from April 2020 to October 2020.

3.2.6 Population of the Study:

The population of this study was data set (brain tumors T2 weighted MR Images), include both gender with all age

3.2.7 Inclusion Criteria:

All patient with intracranial tumor who have MRI scan.

3.2.8 Exclusion Criteria:

All patient with negative contrast enhancement and patient underwent a surgical procedure.

3.2.9 Ethical approval

The ethical approval was granted from the hospital and the radiology department; which include commitment of no disclose any information concerning the patient identification, no patient data were published and the data were kept in personal computer with personal password.

Chapter four

4. Result

Chapter four

4. Result

The main goal of this study to characterize the brain tumors in MR Images, and the characterization of image done by first order statistic Texture Analysis. A 50 T2 weighted MR images for patient diagnosed with brain tumor were clearly analyzed. The result of this study represented in following figures and tables.

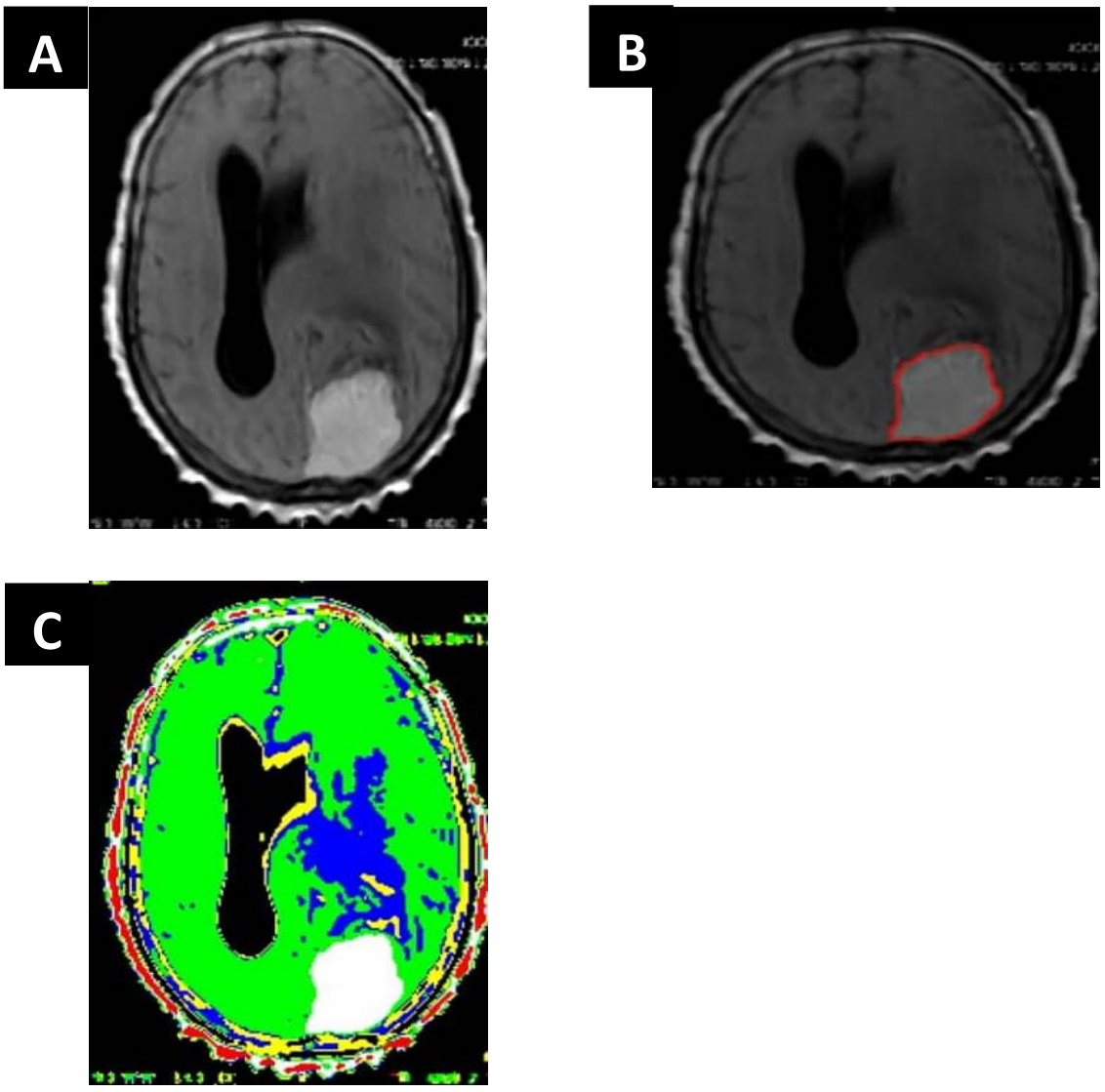

Figure 4.1. Demonstrat MR image (A) the original MR image with contrast demonstrate the brain tumor. (B) Showed the lesion (brain tumor) drawn using

intensity profile of the MR image in which the tumor borders clearly outlined. (C) Shows the calcification map created using selected feature of each class (Brain tissue (Gray and White matter), brain tumor, CSF and fatty tissue).

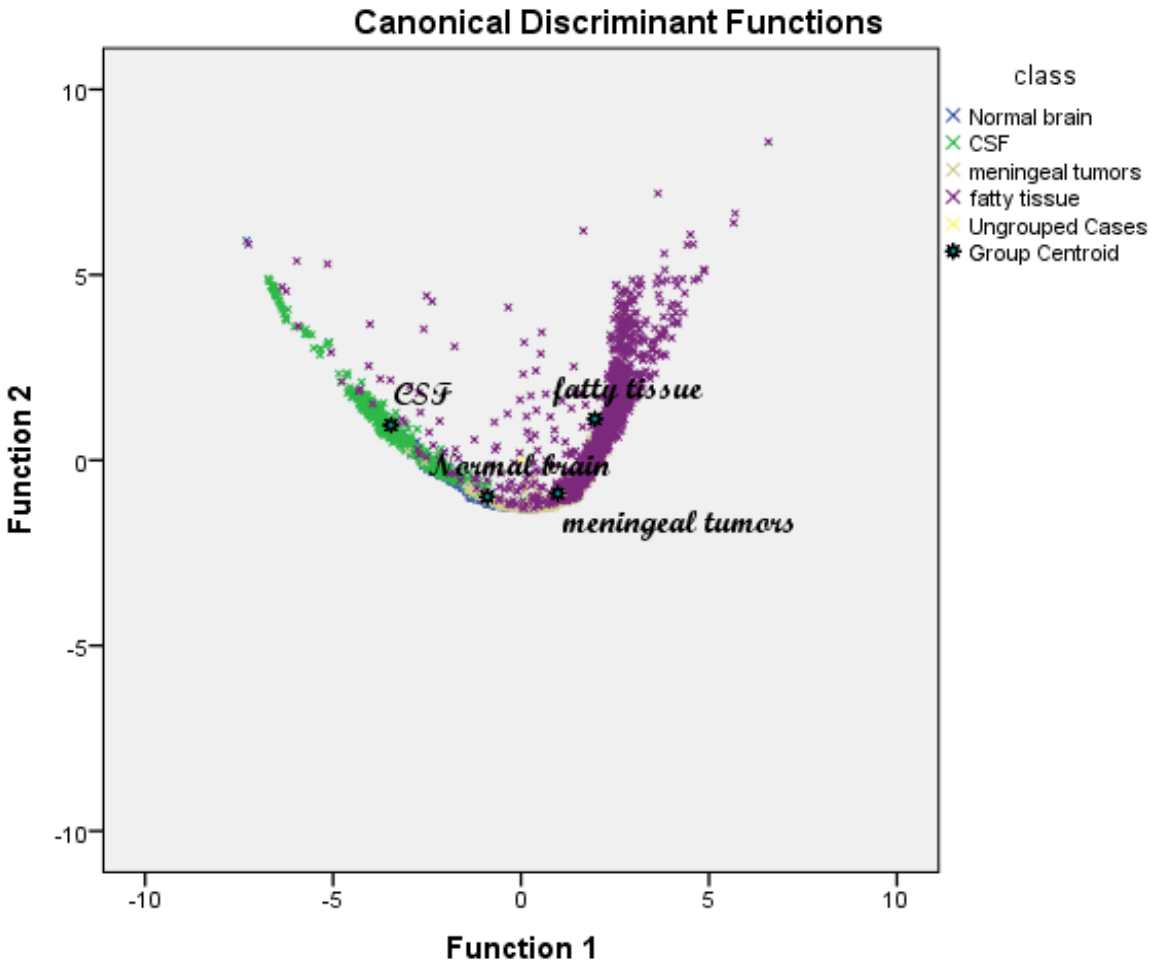

Figure 4.2 show Scatter plot generated using discriminate analysis function for four classes represents: normal brain tissue, CSF, brain tumor, fatty tissue.

	Class	Predicted Group Membership				Total
		Normal brain	CSF	Brain tumors	fatty tissue	
%	Normal brain	**89.6**	2.7	7.7	.0	100.0
	CSF	17.5	**82.5**	.0	.0	100.0
	Brain tumors	11.6	.2	**80.8**	7.4	100.0
	fatty tissue	3.9	2.7	21.5	**71.9**	100.0

Table 4- 1 classification accuracy of the brain tumor using linear discriminant analysis**.**

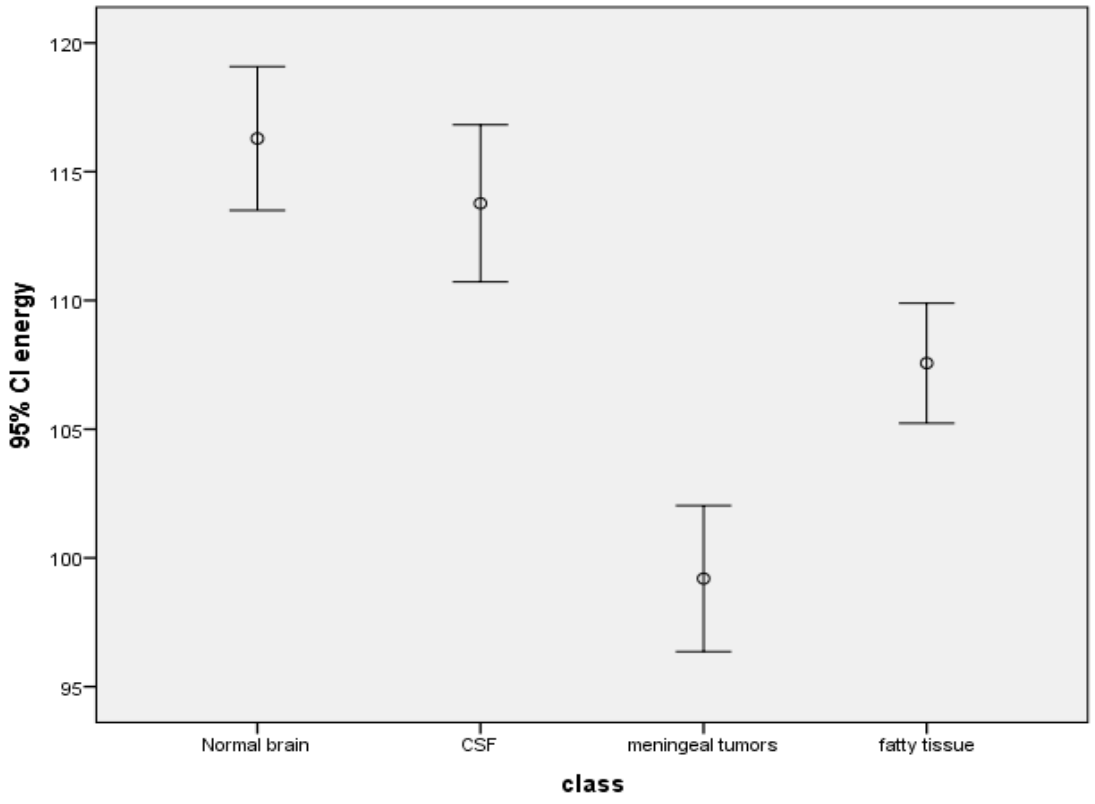

Figure 4.3 Simple error bar graph showed the classification based on energy for MR image (normal brain, brain tumors, CSF, fatty tissue)

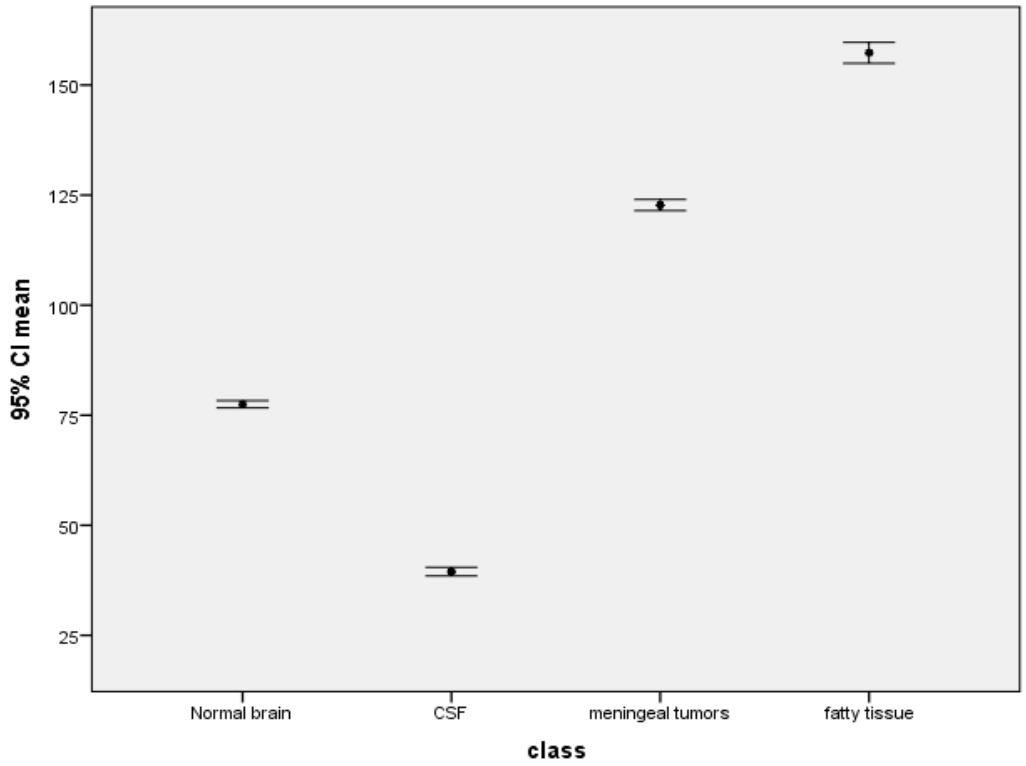

Figure 4.4 Simple error bar graph showed the classification based on mean for MR image**.**

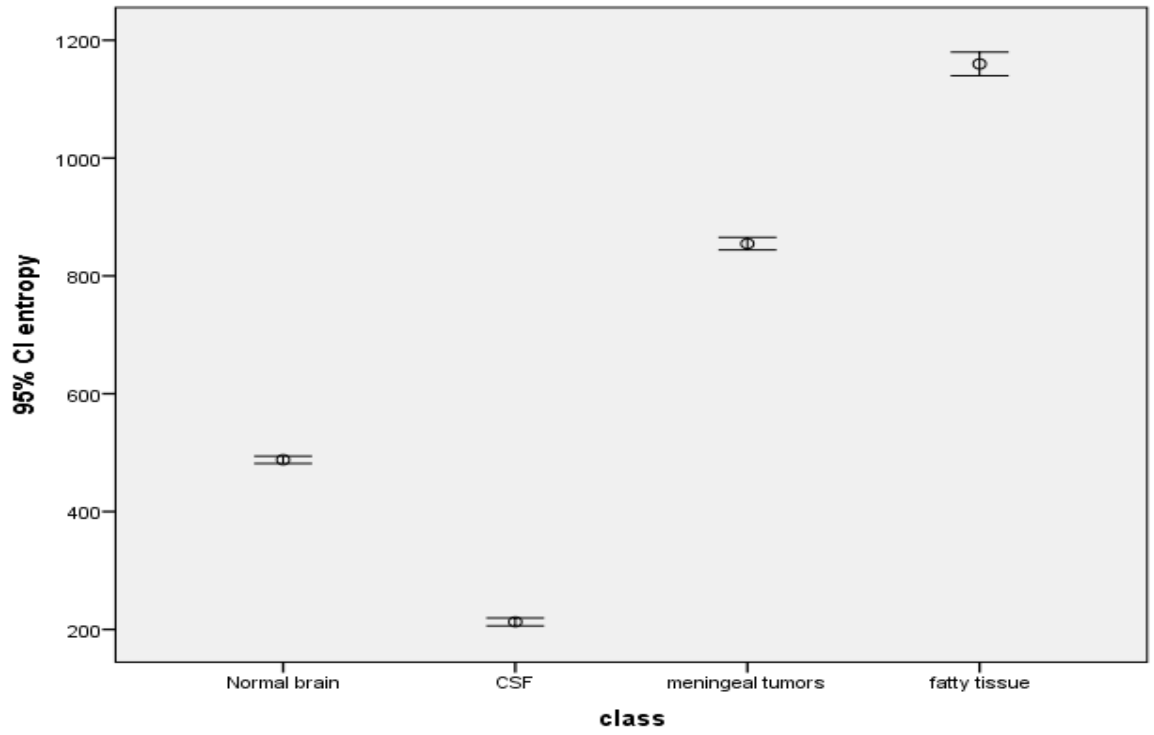

Figure (4.5) Simple error bar graph showed the classification based on entropy for MR image.

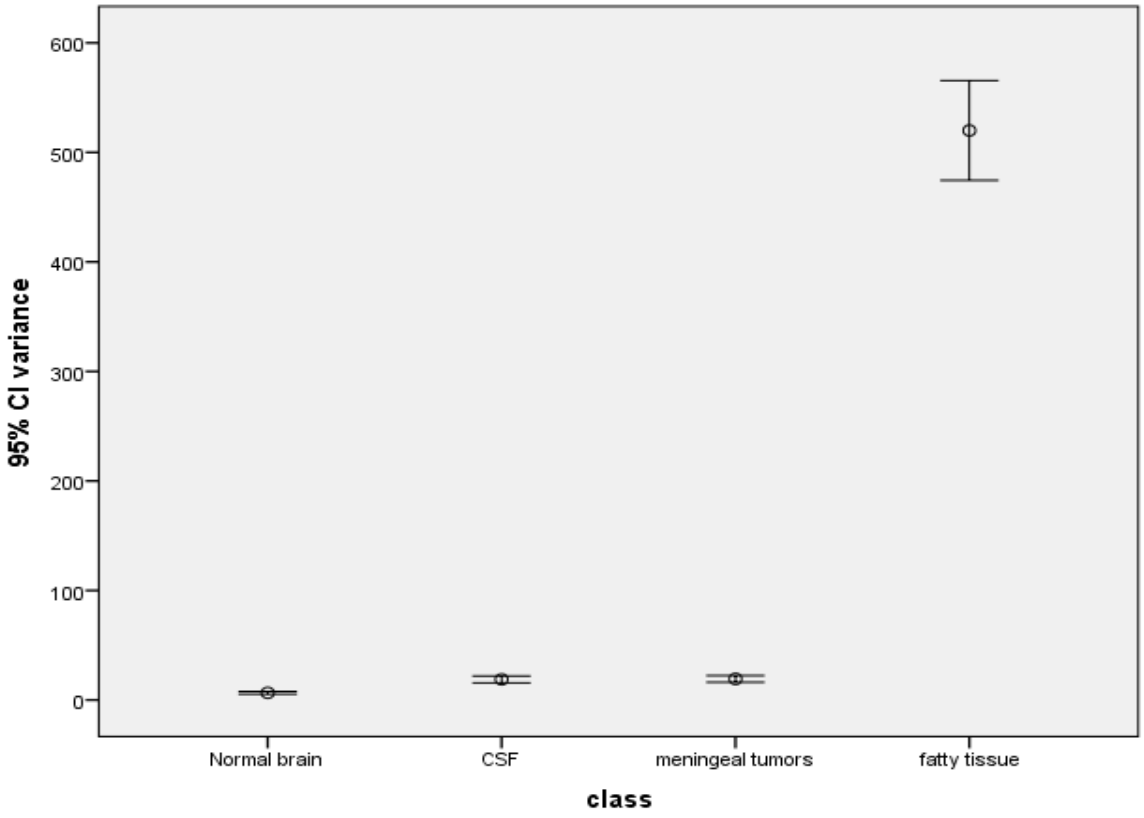

Figure 4.6 Simple error bar graph showed the classification based on variance for MR image.

Chapter Five

5.1 Discussion

Chapter Five

5.1 Discussion

Texture analysis was presented here as a useful computational method for discriminating between pathologically different regions on medical images because it has been proven to perform better than human eyesight at discriminating certain classes of texture [(11)]. Presents statistical texture analysis through first order feature techniques. Extracted from the images for five selected brain MRI sequences in order to test which is better for classification and brain meningeal tumor characterization using different window sizes which were 3x3 pixel window size was finally selected. These feature included: FOS texture (mean, energy, entropy, variance) these feature were calculated for four different classes which were: (normal brain tissue, CSF, fatty tissue and brain tumor).

In this study we use different variable (Energy, mean, entropy, variance) to classify texture feature of the brain tumor.One of the most important aim of this study was to draw the GTV for brain tumor as final study result based on both extracted texture and intensity profile relative brain tissue and generation of classification map. (figure 4.1). The classification Map that created using linear discriminant analysis functions from four different tissue classes of brain tissue, CSF, fatty tissue and brain tumor are clearly separated according to calculated texture at $P<0.05$, and CL=95%. Also there was some similarity noted between tumor and brain tissue possibly due to good tissue differentiation especially for small size (early stage) tumors in which cancer tissue relatively similar to the tissue of organ morphologically. But CSF were clearly discriminated because it has a small pixels intensity and low MR intensity signals. (Figure 4.2.), 80.7 % of original grouped cases correctly classified for 3x3 window generated using step-wise technique to select the most significant feature that can be used for purpose of tumor characterization which are: difference average of SGLD, energy, mean, entropy and variance from first order statistics. (Table 4-1). In case

of the energy, mean and entropy, brain tumor was clear difference from the normal tissue and CSF, while there was some similarity noted between tumor and fatty tissue (Figure 4.3 , 4.4 , 4.5), but in case of variance the brain tumor was clearly discriminated from the fatty tissue ,however, No clear difference from the brain tissue and CSF. (Figure 4.6.).

5.2 Conclusions:

Brain tumors is one of the major health problem today that affect majority of both younger and adults people all over the world, this study were carried out to characterize the brain tumor in Sudanese population by introduction of new method of CAD which known as texture analysis technique which used for extracting the information from the images using different techniques using simple matrix with different sizes. Extracting the information from these matrices using textural features, which are sensitive to specific elements of texture, provides unique information on the structure of the texture being investigated. Haralick et al (14) proposed a set of local features specifically designed for this purpose Haralick et al (14). An analytical case control study underwent MRI scan using SIGNA-GE MR scanner for 5 patient with brain tumor, in Antalia Medical Center in period from April to August 2020, different textural feature was extracted using 3x3 matrix window, which are FOS feature for normal and cancerous samples, and the result showed that FOS selected feature was used for classification using mentioned window sizes, discriminant analysis was used classify the brain tissue; the classification accuracy, sensitivity and specificity for (normal brain tissue , CSF , Fatty tissue and brain tumor) was 89.6% , 82.5% , 71.9% , 80.8% respectively at ($P<0.05$, and CL=95%). The result showed that (3x3) having higher classification accuracy than the rest possible because of small dynamic range of useful MRI images, the feature selected for classification from 3x3 window; were mean of gray level of image histogram, and entropy.

Normal tissue= (mean*6.610) + (variance*0.003) + (energy*0.054) + (entropy*-0.783) -69.478

Brain tumor =(mean*7.056) + (variance*0.004) + (energy*0.041) + (entropy*-0.829)-82.314

CSF = (mean * 4.853) + (variance * 0.002) + (energy * 0.056) + (entropy *-0.579) – 38.741

Fatty tissue=(mean*6.416) + (variance*0.007) + (energy*0.043) + (entropy*0.745)-78.450

5.3 Recommendations

Texture analysis can be carried out in all axial image where the tumor were visible in order to delineate the tumor outline for rendering or having the volume of the tumor. Further study could be done to differentiate between the type of brain tumors.

Adoption of such type of program by radiology department can facilitate a lot of useful information about the region of interest. Initiation of image processing unit in the radiology department can help a lot in activation of image processing projects Further classification of the brain that associated with intra cranial disease.

5.4. References

- V. Bruce et al (2003), Visual Perception: Physiology, Psychology and Echology.
- H. Symonds et al (1994), Induction Versus Progression of Brain Tumor Development Differential Functions for the PRB and P53Targeting Domains of Simian Virus 40 T Antigen.
- B. Charlotte et al (2010), Uterine Sarcoma – Current Perspectives.
- C.D Kubicky et al (2010), Characterization of Brain Gilioma in Magnetic Resonance Images Using Texture Analysis Techniques.
- Medical Imaging in Cancer Care (2012).
- H.C Chen et al (1998), The Handbook of Pattern Recognition and Computer Vision, 2nd Edition, World Scientific Publishing Co, pp 3 – 8.
- H. Harms et al (1986), Combined Local Color and Texture Analysis of Stained Cells.
- Gelsema and Landeweerd (1978), The Use of Nuclear Texture Parameter in the Automatic Analysis of Leukocytes.
- M.F. Insana et al (1986), Analysis of Ultrasounds Image Texture Via Generalized Rician Statistics.
- W. Nailon (2010), Texture Analysis Methods for Medical Image Characterization, Biomedical Imaging, Youxin Mao (Ed.), Intech , pp 80 – 83.
- J.K. Keller et al (1989), Texture Description and Segmentation Through Fractal Geometry, Academic Press.
- R.M. Haralick (1993), Textural Features for Image Classification.
- W. Therrien et al (1989), Cluster Sctructure Evaluation of Dyadic Kmeans Algorisms for Mining Large Image Archives.
- Jain and D. Zongker (1997), Feature Selection: Evaluation, Application, and Small Sample Performance.
- A.K. Jain and B. Chandrackaran (1982), 39 Dimensionality and Sample Size Considerations in Pattern Recognition Practice.
- P.A. Devijver and J. Kittler (2012), Pattern Recognition: Theory and Applications.
- J. Nouza (1995), on the Speech Feature Selection Problem: Are Dynamic Features More Important Than the Static Ones?
- J.A. Hartigan (1975), Printer Graphics for Clustering.

- J.L. Duda et al (2001), Perspectivas De Meta De Los Adolescents En El Context Academico.
- P.T. Meyer et al (2017), Comparison of 68Ga-HBED-CC PSMA-PET/CT and Multiparametric MRI for Gross Tumor Volume Detection in Patients with Primary Prostate Cancer Based on Slice by Slice Comparison with Histopathology.
- M.L. Welton et al (2001), Local Therapy for Rectal Cancer.
- R. Steenbakkers et al (2005), Target Definition in Prostate Head and Neck.
- B.B. Mandelbrot (1977), Lecture V: Fractals and Turbulence: Attractors and Dispersion.
- L. Hassan et al (2016), Multi Texture Analysis of Colorectal Cancer Continuum Using Multi Spectral Imagery.
- Hammad et al (2010), Medical Image Understanding and Analysis
- Pantelis (2000), Real Time Rendering of 3D Clouds.
- E.E. Solomou et al (2008), Improving Brain Tumor Characterization on MRI by Probabilistic Neural Networks and Non-Linear Transformation of Texture Features.

Appendix

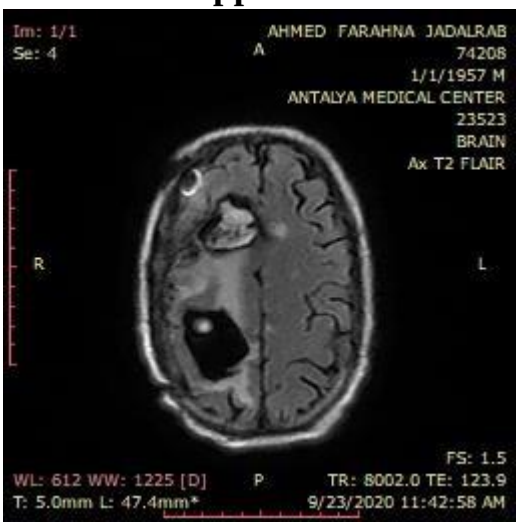
Im: 1/1
Se: 4
A
AHMED FARAHNA JADALRAB
74208
1/1/1957 M
ANTALYA MEDICAL CENTER
23523
BRAIN
Ax T2 FLAIR
R
L
FS: 1.5
WL: 612 WW: 1225 [D]
P
TR: 8002.0 TE: 123.9
T: 5.0mm L: 47.4mm*
9/23/2020 11:42:58 AM

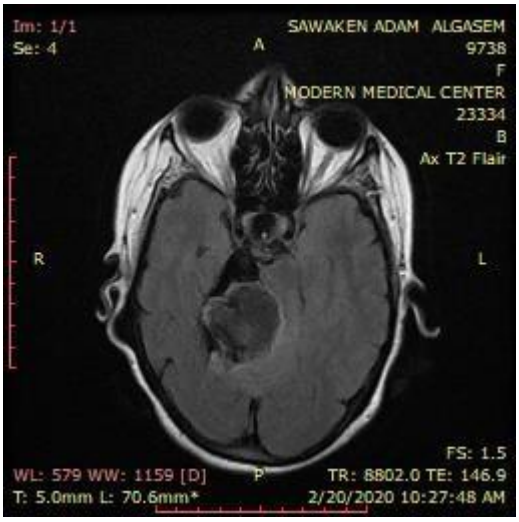
Im: 1/1
Se: 4
A
SAWAKEN ADAM ALGASEM
9738
F
MODERN MEDICAL CENTER
23334
B
Ax T2 Flair
R
L
FS: 1.5
WL: 579 WW: 1159 [D]
P
TR: 8802.0 TE: 146.9
T: 5.0mm L: 70.6mm*
2/20/2020 10:27:48 AM